SAND2023-03985C

Sandia National Laboratories

FLEXO: Next Generation Capabilities for Pulsed Power Experimental Design

Kris Beckwith; Sandia National Laboratories

FLEXO team: Thomas Voth, Stephen Bond, Alan Stagg, Brian Granzow, Nathaniel Hamlin, Matthew Martin, Thomas Gardiner, Marrisa Adams, Jeff Woolstrum, Matthew Weis & Gabriel Shipley

Programmatic & Funding Support: Luke Shulenburger & Steve Bova

U.S. DEPARTMENT OF ENERGY NNSA

Sandia National Laboratories is a multimission laboratory managed and operated by National Technology & Engineering Solutions of Sandia, LLC, a wholly owned subsidiary of Honeywell International Inc., for the U.S. Department of Energy's National Nuclear Security Administration under contract DE-NA0003525.

Sandia National Laboratories ENERGY NNSA

Sandia National Laboratories is a multimission laboratory managed and operated by National Technology & Engineering Solutions of Sandia, LLC, a wholly owned subsidiary of Honeywell International Inc., for the U.S. Department of Energy's National Nuclear Security Administration under contract DE-NA0003525.

Inertial Confinement Fusion (ICF) is an exciting field of research and one of high importance to the DOE/NNSA mission space

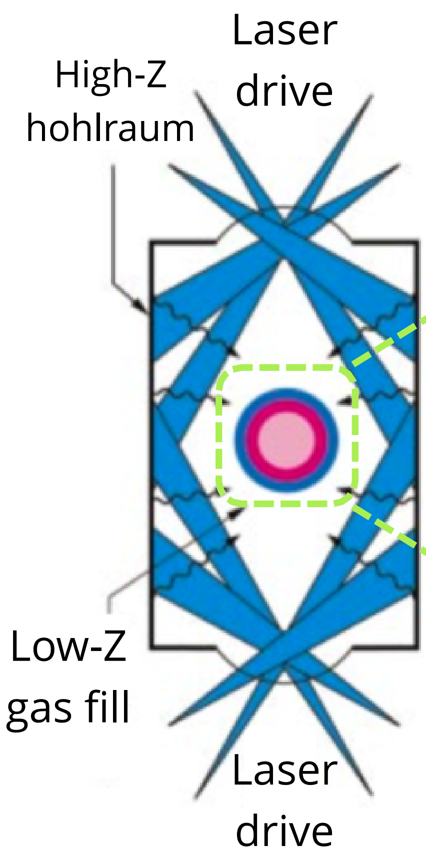

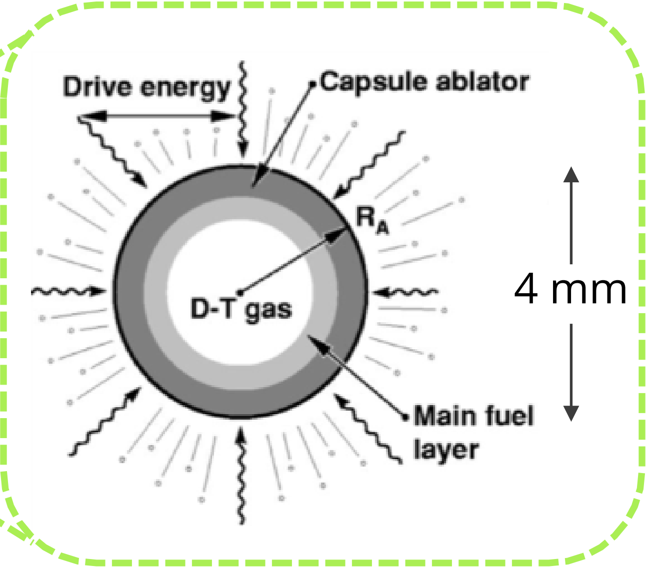

Controlled thermonuclear fusion has applications in:

- Nuclear weapons stockpile stewardship
- Radiation effects science
- Energy production

Lindl et al., POP 11, 339 (2004), Clark et al., PPCF 59, 055006 (2017)

Sandia National Laboratories

- Long history of expertise and leadership in pulsed power accelerator science and technology.
- Sandia's Magnetized Liner Inertial Fusion approach seeks to achieve thermonuclear conditions in pulsed-power-driven cylindrical implosions.

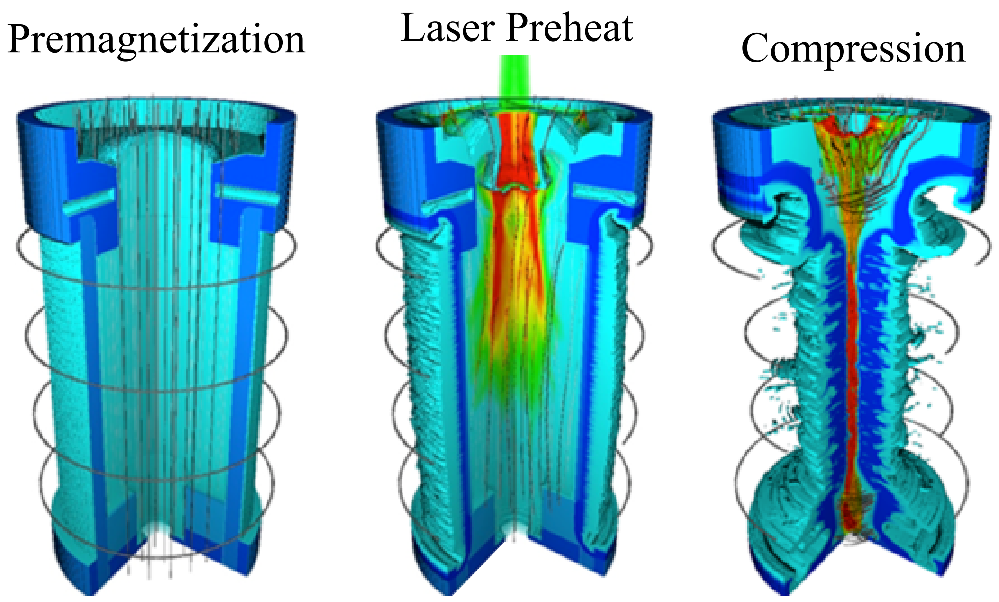

S. A. Slutz et al., Phys. Plasmas **17**, 056303 (2010).

The Z accelerator (the "Z Machine") is the largest and most powerful pulsed power accelerator in the world

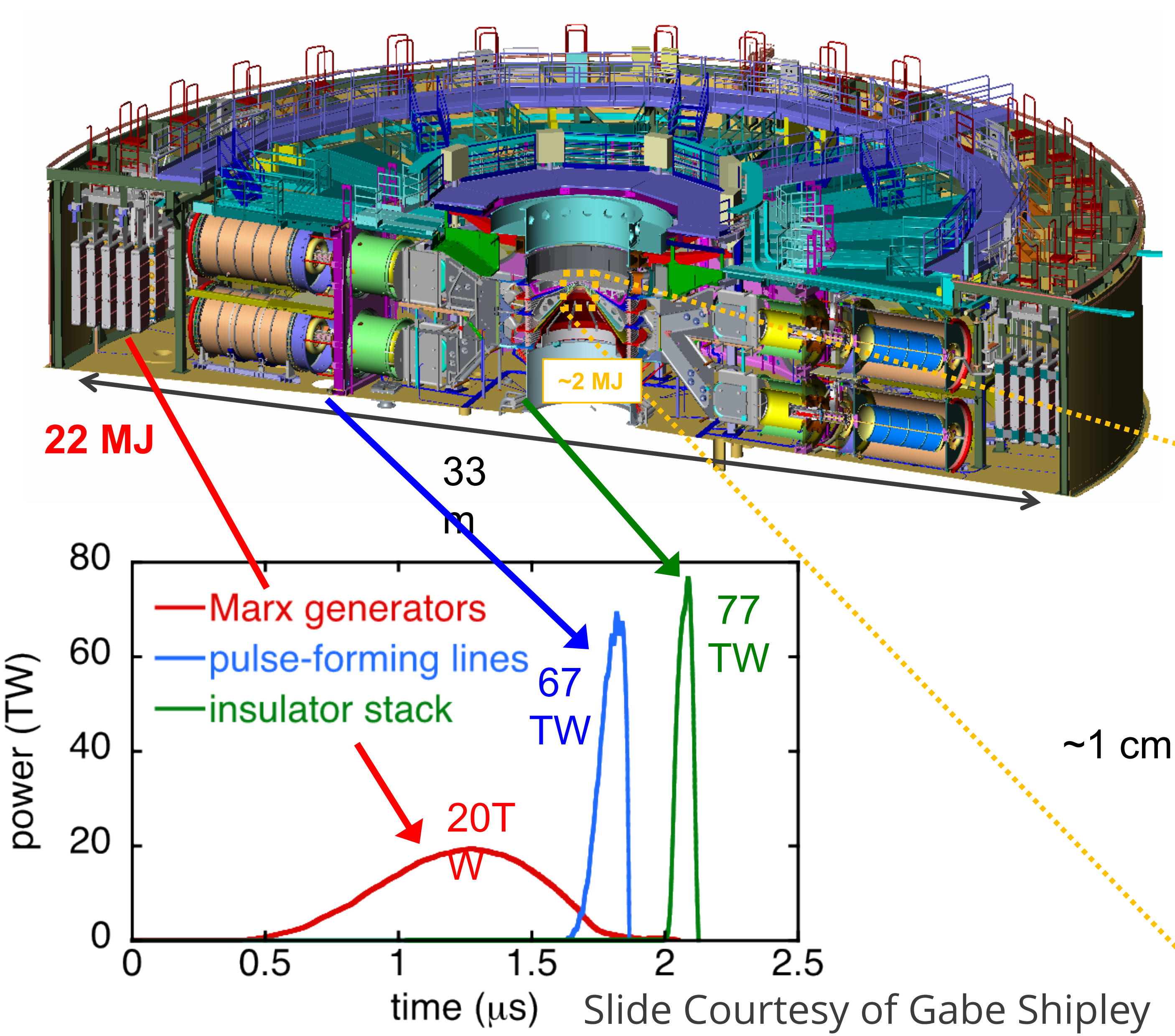

Slide Courtesy of Gabe Shipley

Sandia National Laboratories

- Long history of expertise and leadership in pulsed power accelerator science and technology.
- Sandia's Magnetized Liner Inertial Fusion approach seeks to achieve thermonuclear conditions in pulsed-power-driven cylindrical implosions.

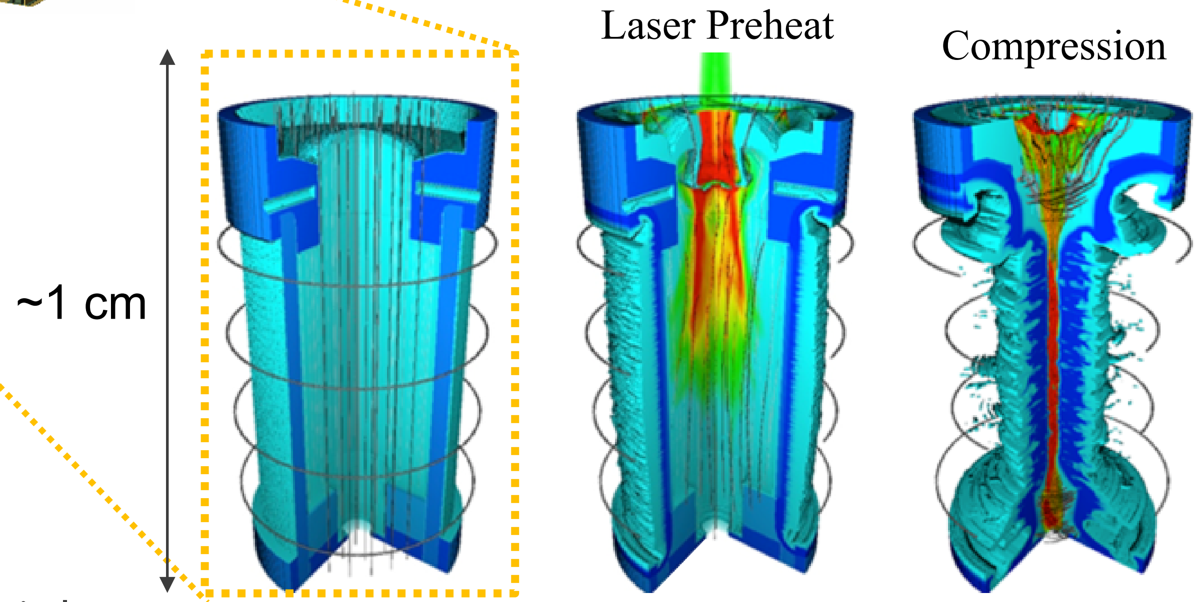

S. A. Slutz et al., Phys. Plasmas **17**, 056303 (2010).

Magnetized Liner Inertial Fusion (MagLIF[1]): Magnetic compression of premagnetized, laser-preheated fusion fuel

Slide Courtesy of Gabe Shipley

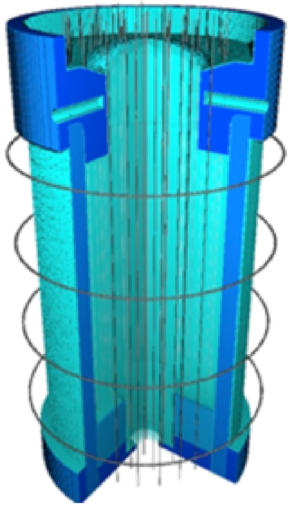

- **Premagnetization[2]: 10-20 T quasi-static axial magnetic field, $B_{z,0}$, is applied to thermally insulate fuel**

Reduces required implosion velocity compared to laser ICF

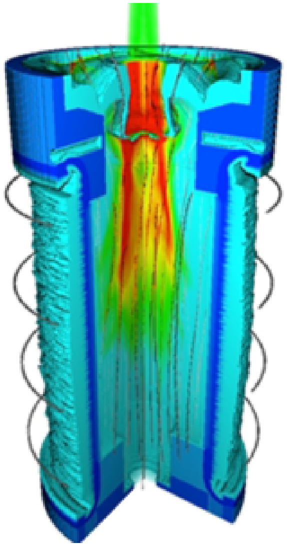

- **Laser preheat[3]: The fuel is pre-heated using the Z-Beamlet Laser (4 kJ)**

Reduces required compressive heating compared to laser ICF

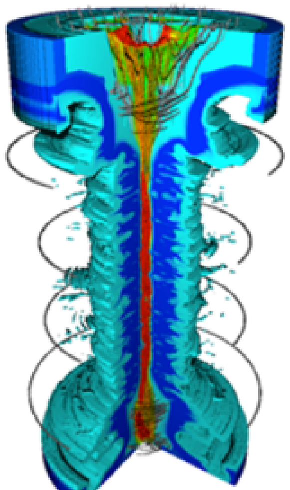

- **Compression: Z Machine drive current implodes liner, ~18 MA in 100 ns**
  - **Adiabatically compresses fuel to thermonuclear conditions**

Deuterium-gas-filled beryllium liner (cylindrical tube)

[1] S. A. Slutz et al., Phys. Plasmas **17**, 056303 (2010). [2] Rovang et al., Rev. Sci. Instrum. **85**, 124701 (2014). [3] Harvey-Thompson et al., Phys. Plasmas **26**, 032707 (2019).

Each component of MagLIF[1] has unique challenges

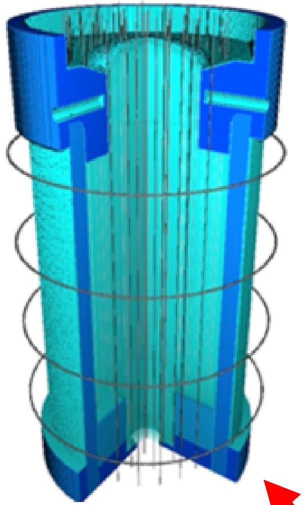

- **Premagnetization[2]**

Background axial magnetic field provided by external field coil system.
Field strength is limited by coil technology.
External coils limit diagnostic access to target.

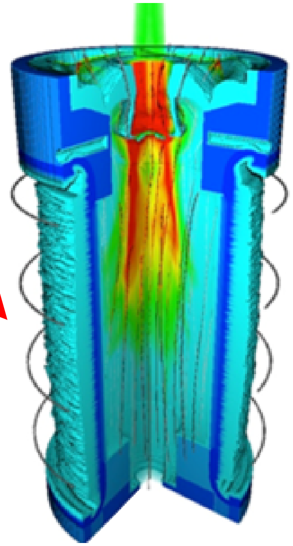

- **Laser preheat[3]**

Laser energy coupling to fuel suffers from losses.
Laser energy deposition can exacerbate liner-fuel material mix (radiative losses).

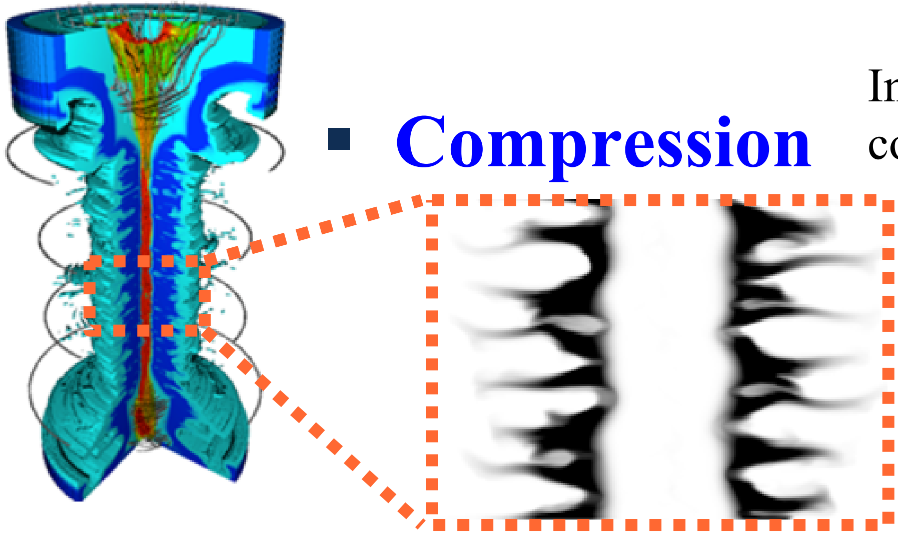

- **Compression**

Instabilities in imploding liner degrade compression of fuel, limiting fusion yield.

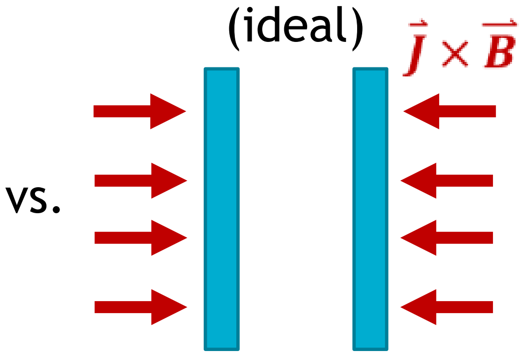

[1] S. A. Slutz et al., Phys. Plasmas **17**, 056303 (2010).   [2] Rovang et al., Rev. Sci. Instrum. **85**, 124701 (2014).   [3] Harvey-Thompson et al., Phys. Plasmas **26**, 032707 (2019).

Modeling the helical instability in magnetized implosions self-consistently remains an outstanding challenge

MHD simulations* have successfully reproduced instability structures comparable to data…

but not in an ab initio fashion, instead requiring an unphysical perturbation seed with an embedded helical correlation.

White noise perturbation on outer liner surface with 7.2° helical bias

20-μm amplitude

Liners have 100-200 nm RMS surface roughness

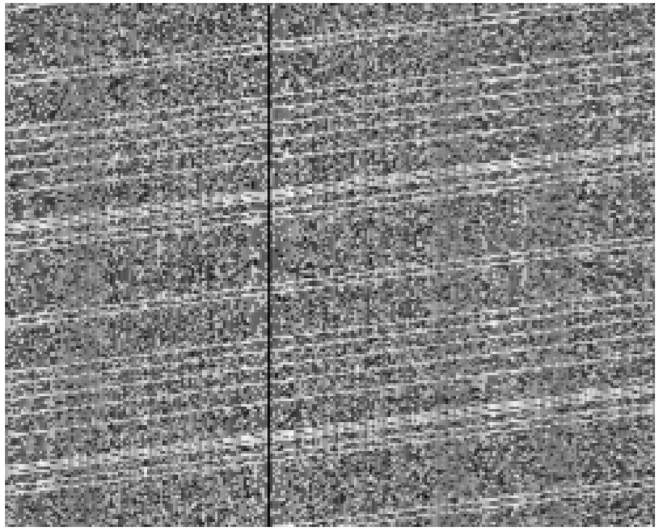

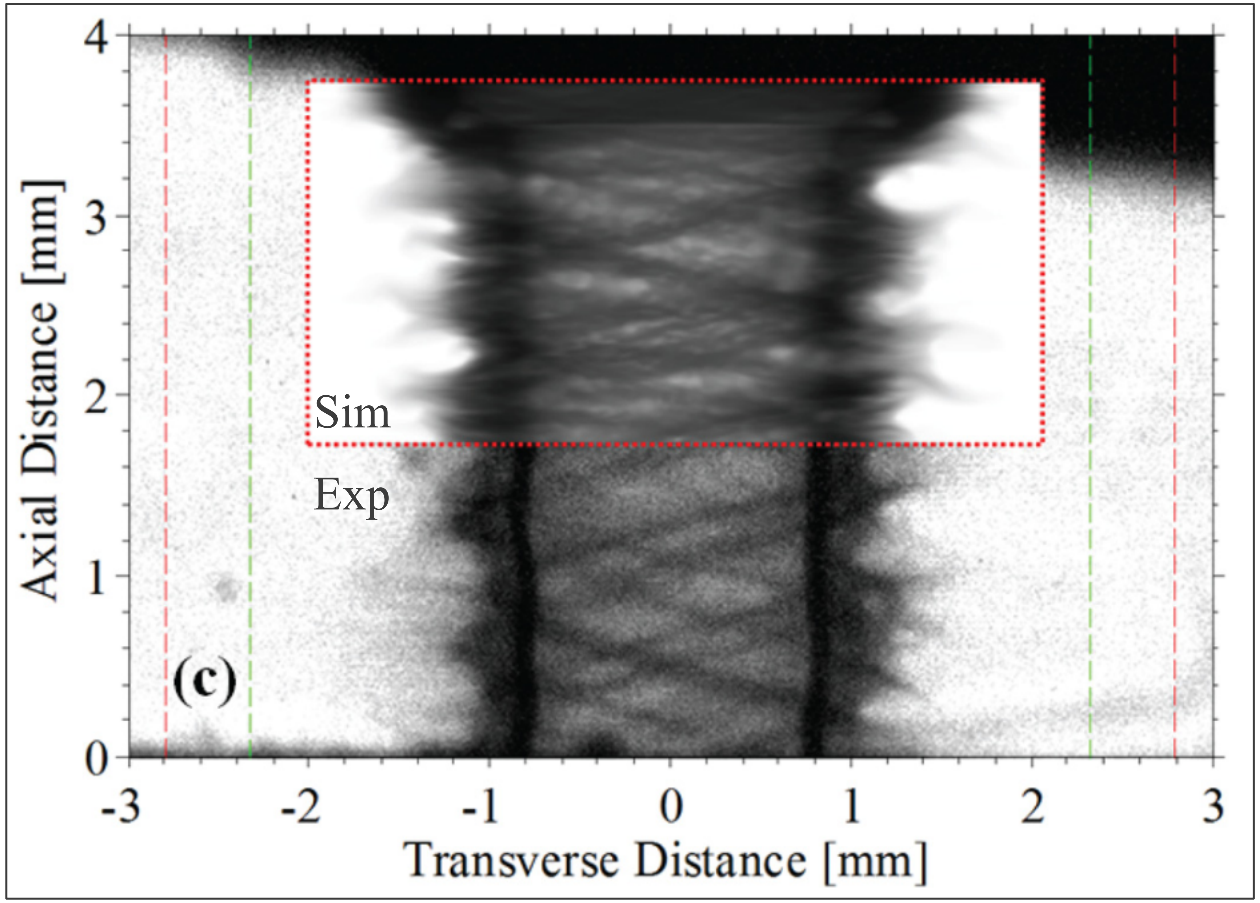

*T. J. Awe et al., *Phys. Rev. Lett.* **111**, 235005 (2013).

Slide Courtesy of Gabe Shipley

Common approach for modelling compression is founded upon resistive MHD approximation which leads to unphysical behavior in vacuum surrounding liner

Static liner surrounded by vacuum
(driven by current rise ~20MA in ~100ns)

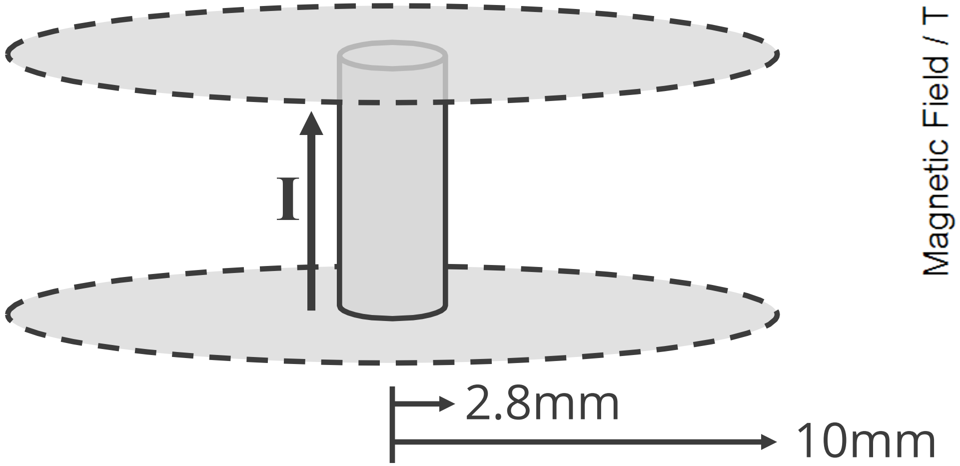

A high vacuum resistivity is needed to obtain a converged magnetic field solution

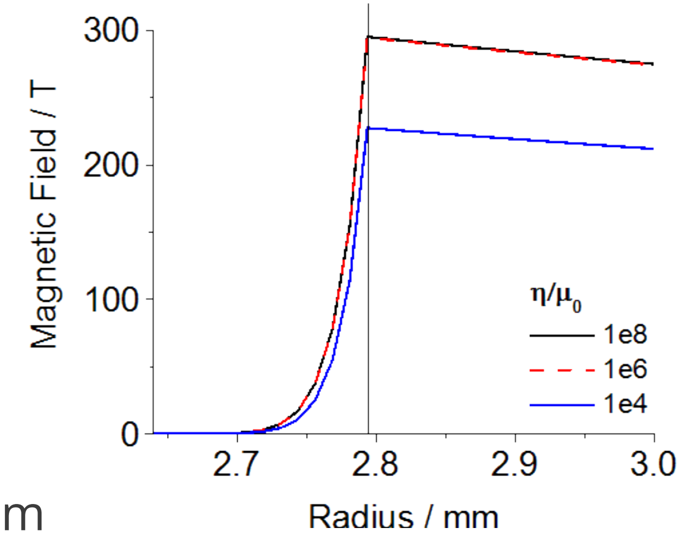

Obtain converged current in metal, but also vacuum current density due to use of RMHD

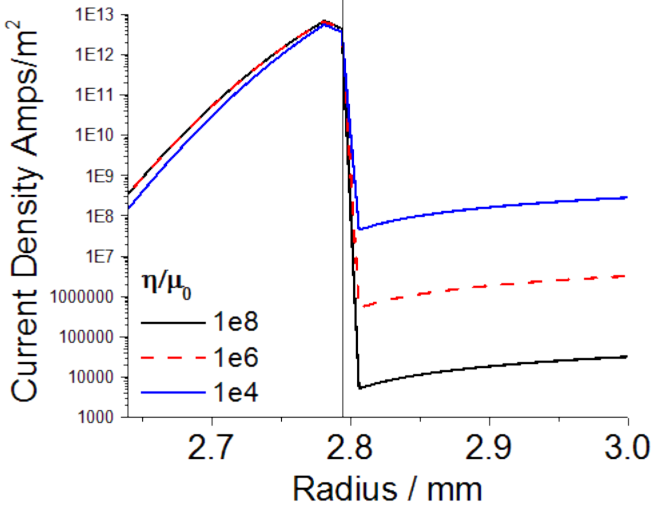

$$\nabla\times E = -\frac{\partial B}{\partial t}$$

$$\nabla\times B = \mu_0 j + \mu_0\varepsilon_0\frac{\partial E}{\partial t}$$

$$E = \eta j$$

$$\nabla\times B = \frac{\mu_0}{\eta}E$$

$$\frac{\partial B}{\partial t} = -\nabla\times\frac{\eta}{\mu_0}\nabla\times B$$

Solve with resistive diffusion approximation
(not applicable in vacuum)

Slide courtesy of Chris Jennings

Unphysical behavior in vacuum surrounding liner is mitigated through adoption of a range of *ad-hoc* model parameters

Current Density

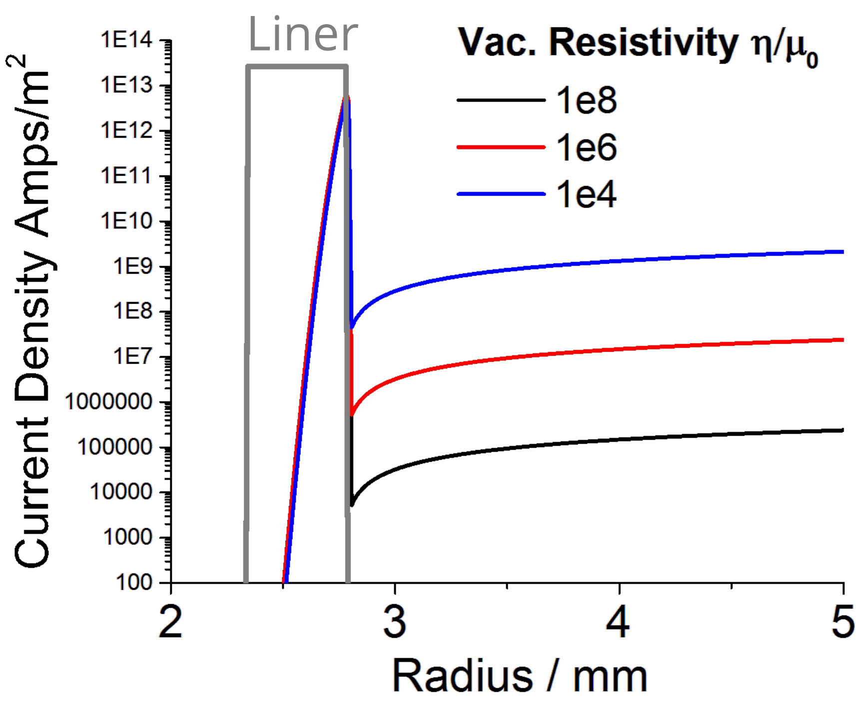

Mass Density

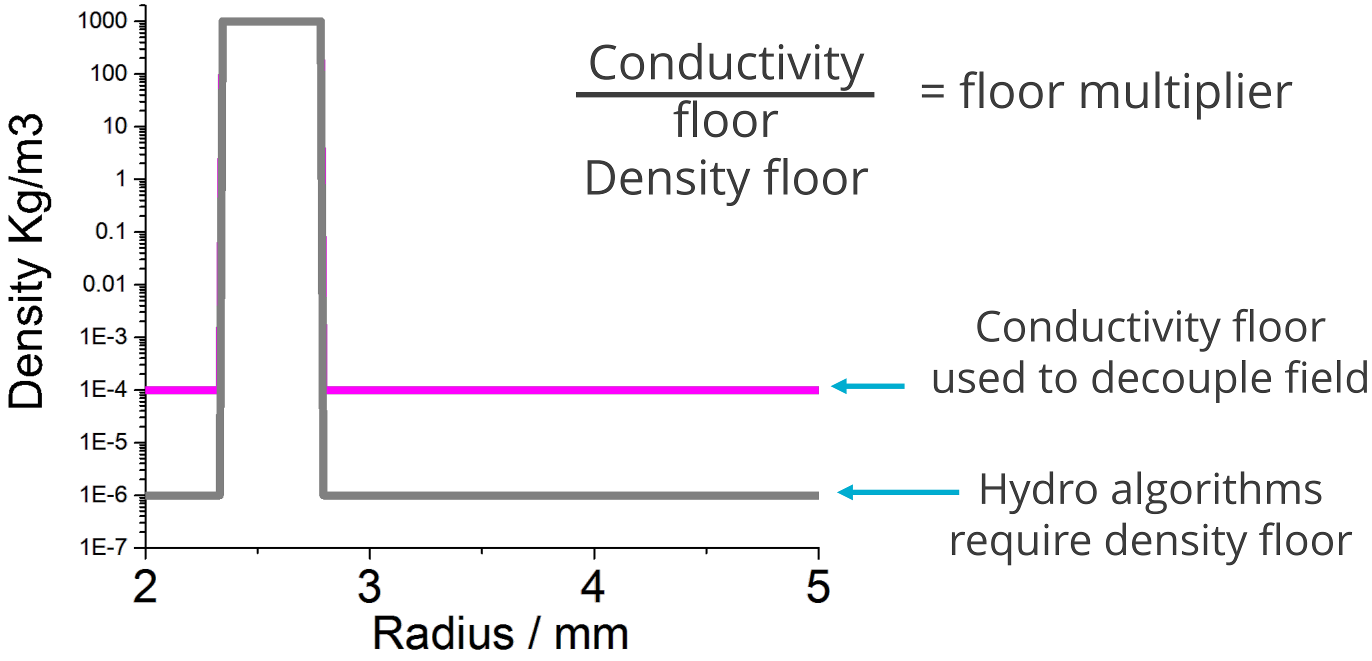

- Current in vacuum is a function of a user defined "vacuum resistivity"
- We want perfect vacuum but hydrodynamics algorithms often require a density floor.
- We don't want material at the density floor to be heated or accelerated by vacuum currents that are only there to allow the field solver to operate
- Define a separate conductivity floor to turn off interactions with vacuum currents

Slide courtesy of Chris Jennings

Choices about *ad-hoc* model parameters determine driver-target coupling and *key performance metrics for the platform*

Eddy-style 1d simulation

Magnetic field

Peak P_{mag}

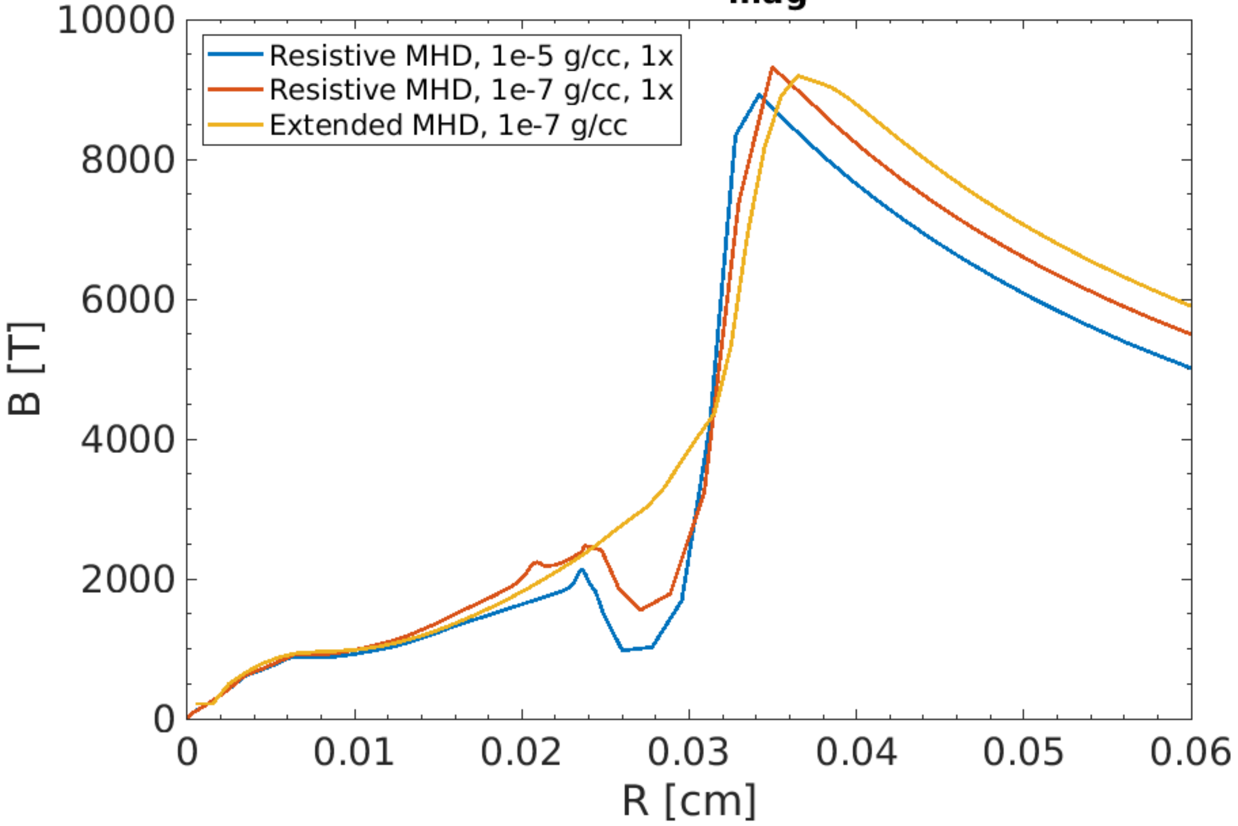

Thermal Pressure

Peak P_{mag}

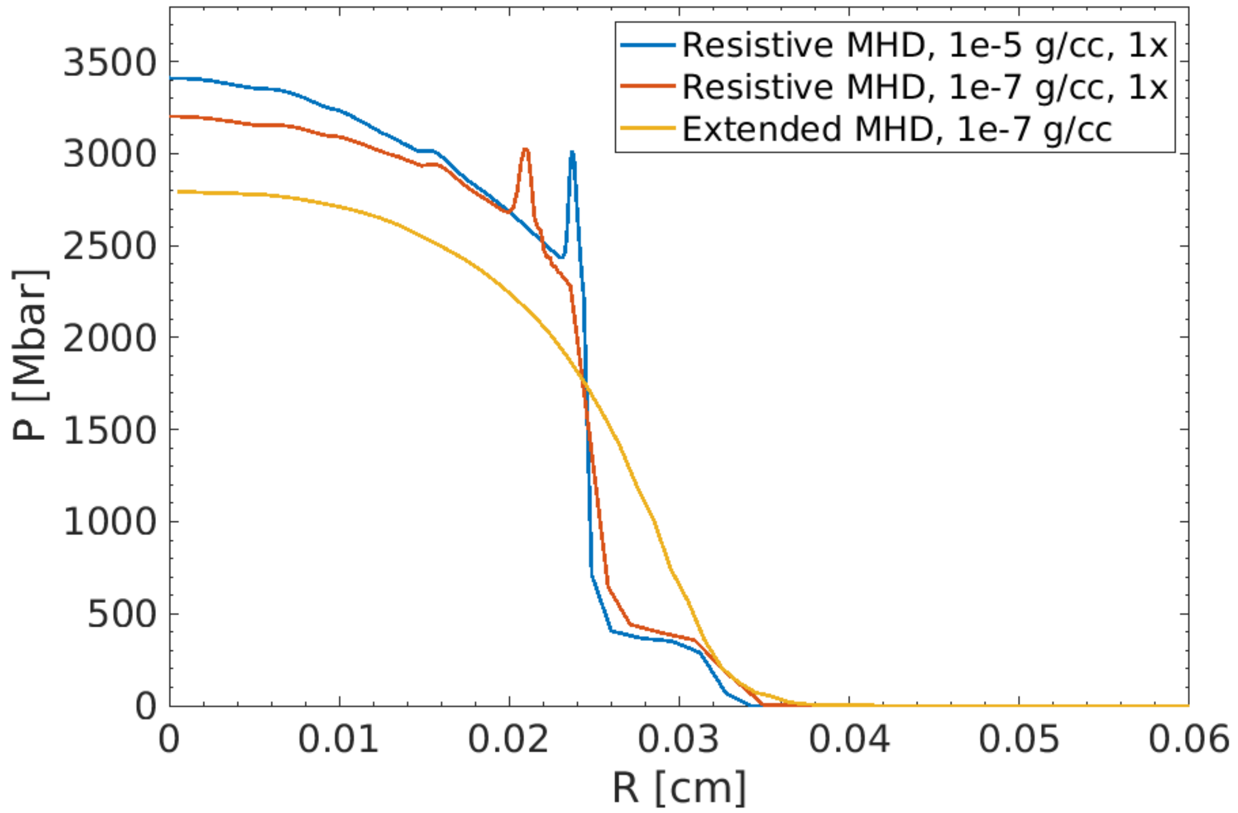

- The physics of how we treat propagation of electromagnetic fields in vacuum is a leading order problem in pulsed power. *Resistive MHD is not predictive for magnetic fields in vacuum and achievable pressures in target*
- Predictive capabilities require us to treat this fundamental physics from an *ab-initio* standpoint **not** using ad-hoc approximations with multiple parameters. *Restoring displacement currents to Maxwell's equations and including physics of electron inertia provides this capability*

Simulations by Matt Weis and Nat Hamlin

SNL are developing new approaches to improve the fidelity of our target design calculations.

- **PERSEUS** – generalized Ohm's Law (XMHD), FORTRAN90, Discontinuous Galerkin (DG) code, originally developed at Cornell (Martin, Seyler) and licensed to SNL with numerous publications demonstrating the need for XMHD physics in the modeling of pulsed power systems.

- **FLEXO** – new C++ XMHD code (Flux Limited EXtended Ohm's law) developed at SNL with new capabilities: multi-material equation of state (EOS), adaptive mesh refinement (AMR), and scalable DG radiation transport, all compatible with advanced architectures (GPU).

Enable a predictive simulation capability for design work on Z and future pulsed power facilities

1) Feed plasma transport requires XMHD due to low densities

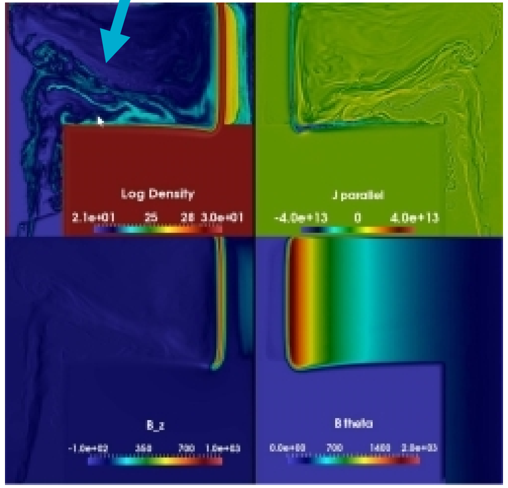

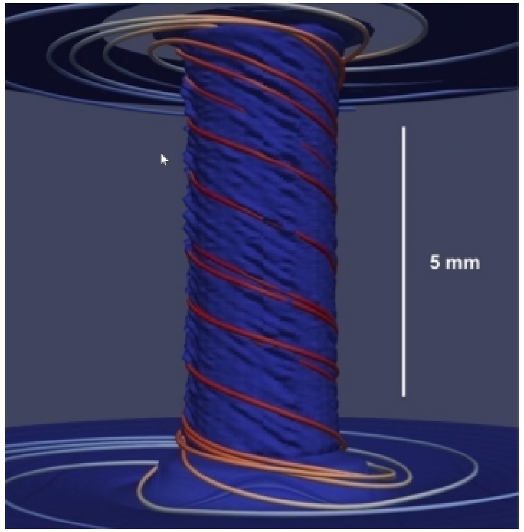

2) XMHD predicts helical instability in 3D calculations due to feed plasma driving flux compression in MagLIF

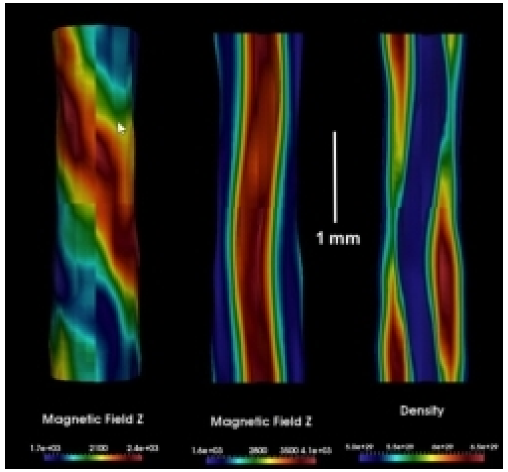

3) Low density feed plasma (~10^18/cc) changes morphology and stability of liner stagnation

New approaches are founded upon Full Maxwell + Generalized Ohm's law + High Order DG

- Governing Equations

$$\partial_t[\rho] + \nabla \cdot [\rho \boldsymbol{v}] = 0,$$

$$\partial_t[\rho \boldsymbol{v}] + \nabla \cdot [\rho \boldsymbol{v}\boldsymbol{v} + p\boldsymbol{I}] = \boldsymbol{J} \times \boldsymbol{B},$$

$$\partial_t[\mathcal{E}] + \nabla \cdot [\boldsymbol{v}(\mathcal{E} + p)] = \boldsymbol{v} \cdot (\boldsymbol{J} \times \boldsymbol{B}) + \eta \boldsymbol{J}^2,$$

$$\partial_t[\boldsymbol{B}] + \nabla \times \boldsymbol{E} = \boldsymbol{0},$$

$$\partial_t[\boldsymbol{E}] - c^2 \nabla \times \boldsymbol{B} = -c^2 \mu_0 \boldsymbol{J},$$

Hall term

$$\partial_t[\boldsymbol{J}] = \frac{n_e e^2}{m_e} \left(\boldsymbol{E} + \boldsymbol{v} \times \boldsymbol{B} - \frac{1}{n_e e} \boldsymbol{J} \times \boldsymbol{B} - \eta \boldsymbol{J} \right).$$

- Discretization Strategy
  - Space: DG P0/P1/P2
  - Time:
    - Fields explicitly advanced to intermediate stage (*), where all source terms except energy are neglected.
    - Implicit (element-local) correction:

$$\boldsymbol{E}^{n+1} = \boldsymbol{E}^* - \Delta t\, c^2 \mu_0\, \boldsymbol{J}^{n+1},$$

$$[\rho \boldsymbol{v}]^{n+1} = [\rho \boldsymbol{v}]^* + \Delta t [\boldsymbol{J} \times \boldsymbol{B}],$$

$$\boldsymbol{J}^{n+1} = \boldsymbol{J}^* + \Delta t \left(\frac{n_e e^2}{m_e} \right) \Big[\boldsymbol{E}^{n+1} + \boldsymbol{v}^* \times \boldsymbol{B}^* - \frac{1}{n_e e} \boldsymbol{J}^{n+1} \times \boldsymbol{B}^* - \eta^* \boldsymbol{J}^{n+1} \Big].$$

For details see: Seyler, Martin, Physics of Plasmas **18**, 012703 (2011)

DG-based multi-material algorithms that can be combined with XMHD physics are being researched and implemented

FLEXO pseudo one-d results agree with analytic solution.

Initial Conditions:

left/inner	right/outer
$\gamma_l = 2$	$\gamma_r = 1.4$
$P_l = 1.$	$P_r = .1$
$\gamma_l = 1.$	$\gamma_r = .125$

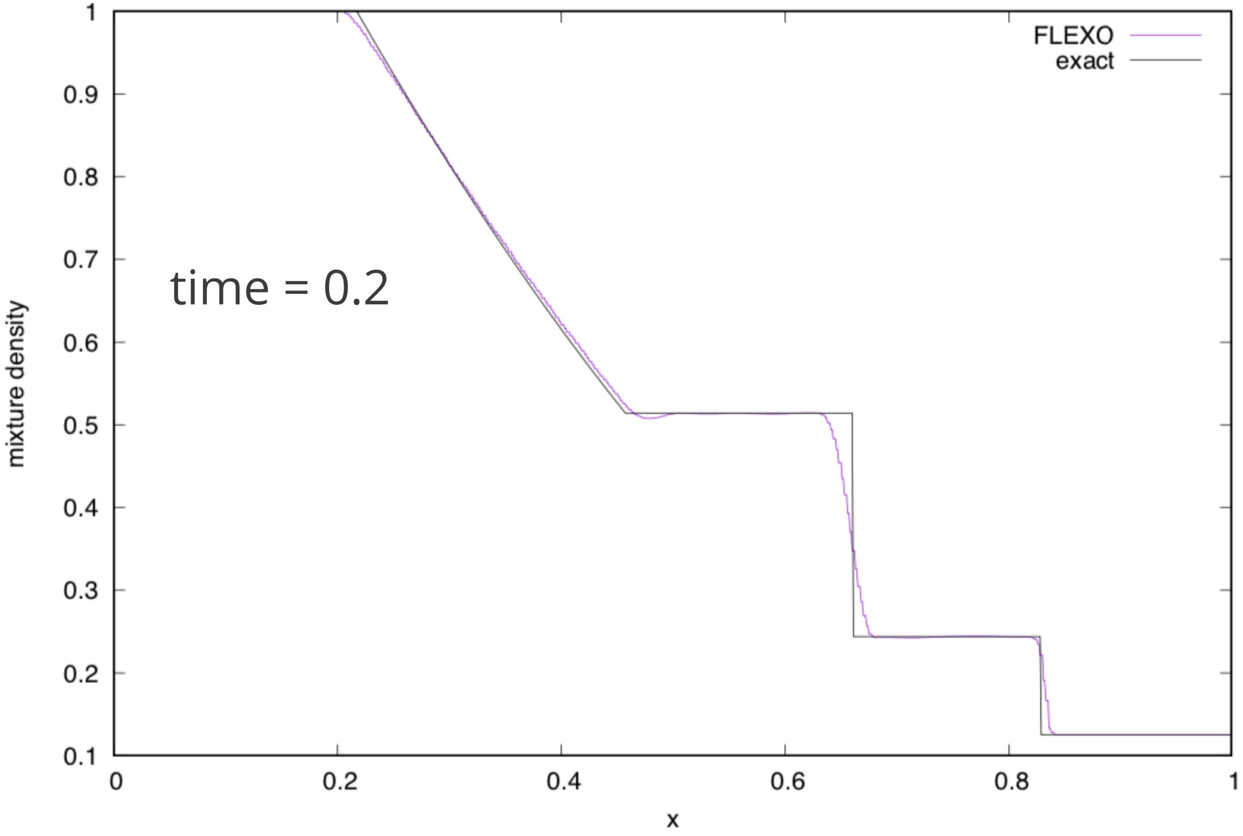

Ideal gas, 100 cells, second order DG

FLEXO produces plausible multi-dimensional multi-material results.

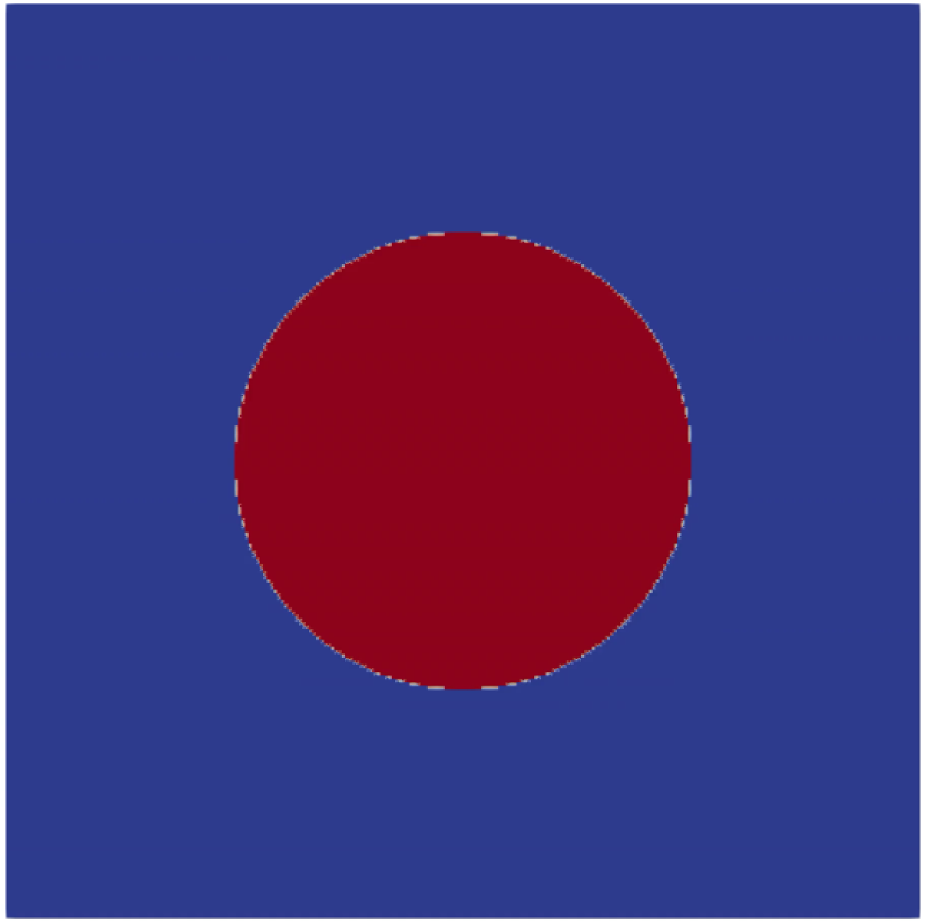

Ideal gas, 65000 cells, second order DG.
GPU wall-clock time (V100): 1 min 45 s

Our code development practices are founded upon rigorous V&V that starts from basic verification problems all the way through to validation…

- Desire a strong V&V culture in development cycle
- TDD/integration in accordance with modern practices (50-ish regression tests. Git controlled code).
- Broad computational physics space must be verified
  - DG -> P0/P1/P2 cells
  - Pure hydrodynamics
  - Pure electromagnetics (EM)
  - Coupled XMHD physics
  - AMR interfaces
  - Execution spaces (GPU/CPU)
- Validation efforts *forthcoming*
  - Match Z experimental results
  - Helical instability with XMHD
  - Integrate PERSEUS validation tests into development cycle

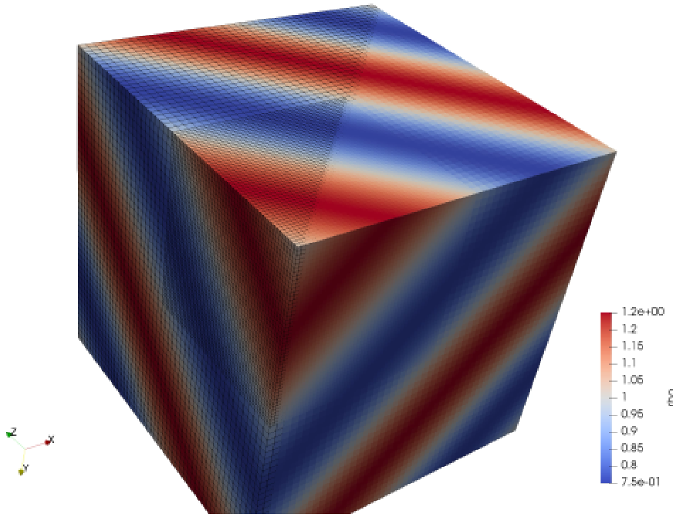

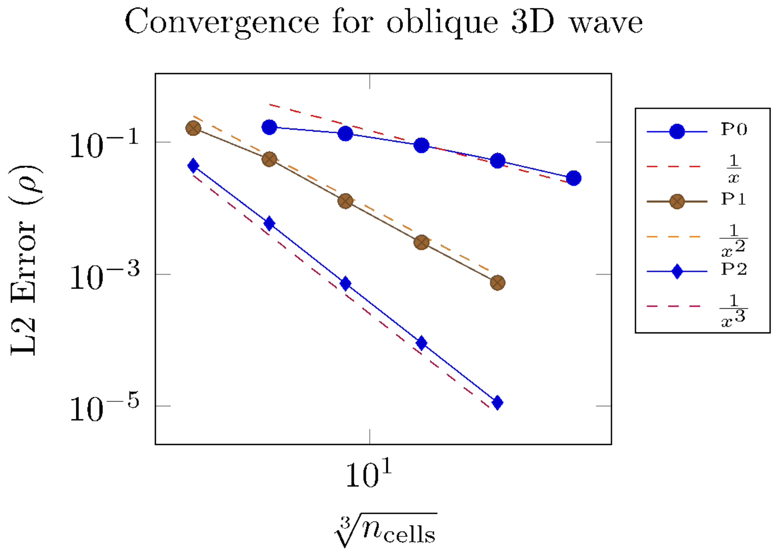

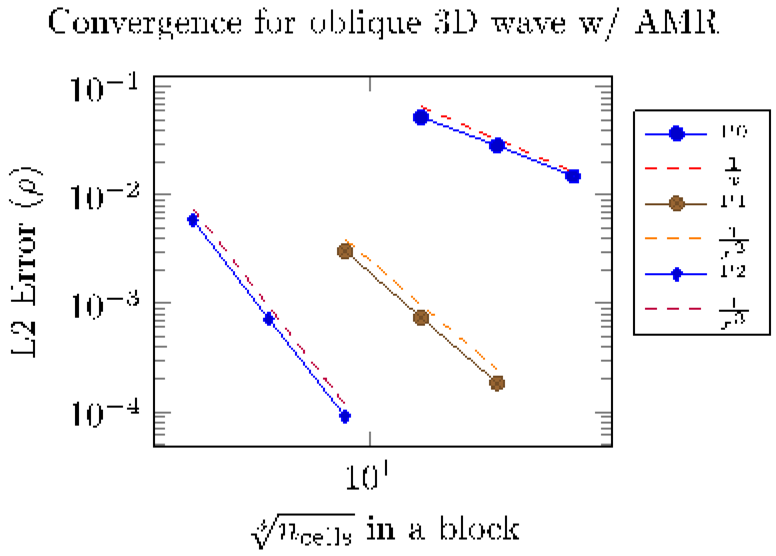

We place emphasis on using these tests to identify bugs and ensure consistency across platforms

- Algorithm development*:

* Voth et al. SAND2020-14220

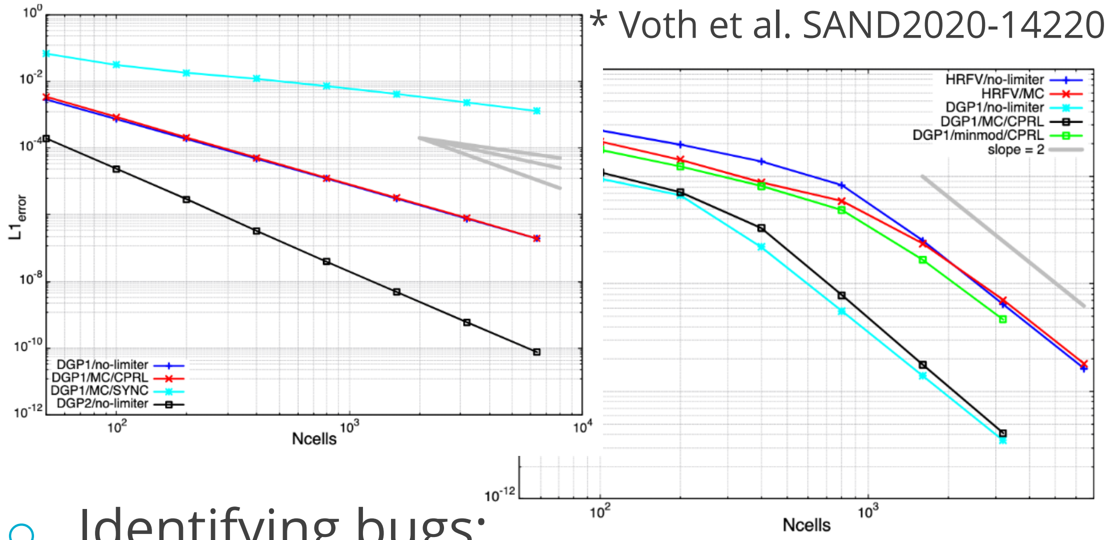

- Identifying bugs:

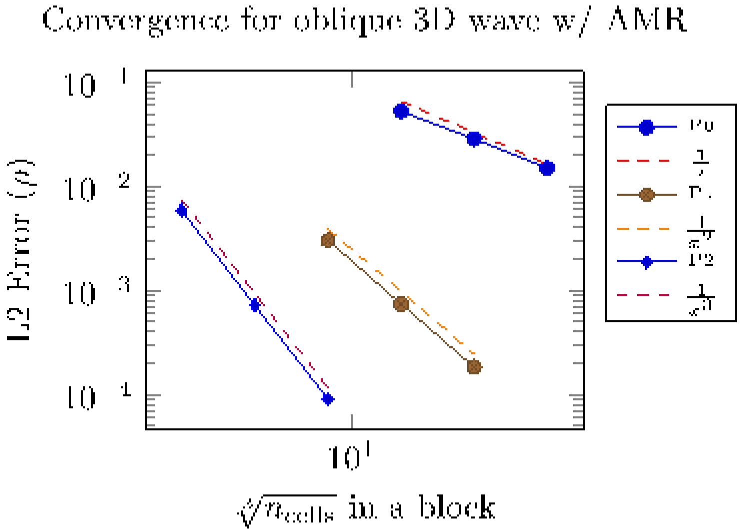

- Ensuring veracity of results on multiple platforms (CPU,GPU):

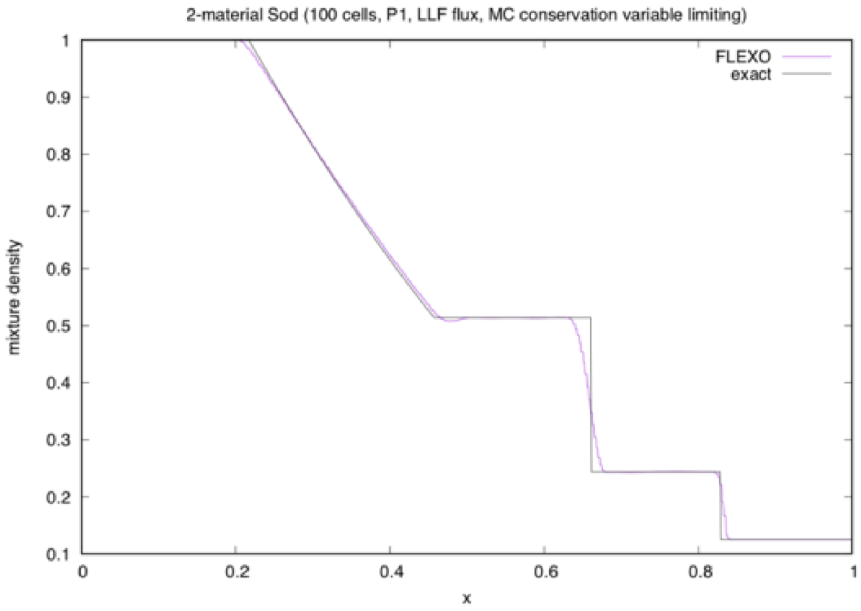

CPU

```
[tevoth@cee-compute012 hydro]$ ./hydro_sod_axis y 1 limited 0.08
9.682470313434e-03      8.858360318252e-03      2.138392848866e-02
4.854880656435e-03      4.280626449299e-03      1.011214287634e-02
[rho]:   computed rate: 9.959393414541e-01 expected rate: 1.000000000000e+00, rel. err: 4.077214722754e-03
[mom]:   computed rate: 1.049217737135e+00 expected rate: 1.000000000000e+00, rel. err: 4.690898313354e-02
[en]:    computed rate: 1.080438165217e+00 expected rate: 1.000000000000e+00, rel. err: 7.444957777943e-02
```

```
[tevoth@vortex27 hydro]$ jsrun --smpiargs="-gpu" --np 1 --nrs 1 --rs_per_host 1 --gpu_per_rs 1 ./hydro_sod
9.682470313434e-03      8.858360318252e-03      2.138392848866e-02
4.854880656435e-03      4.280626449299e-03      1.011214287634e-02
[rho]:   computed rate: 9.959393414540e-01 expected rate: 1.000000000000e+00, rel. err: 4.077214722827e-03
[mom]:   computed rate: 1.049217737135e+00 expected rate: 1.000000000000e+00, rel. err: 4.690898313351e-02
[en]:    computed rate: 1.080438165217e+00 expected rate: 1.000000000000e+00, rel. err: 7.444957777938e-02
```

GPU

We are rapidly moving to a dynamic AMR capability

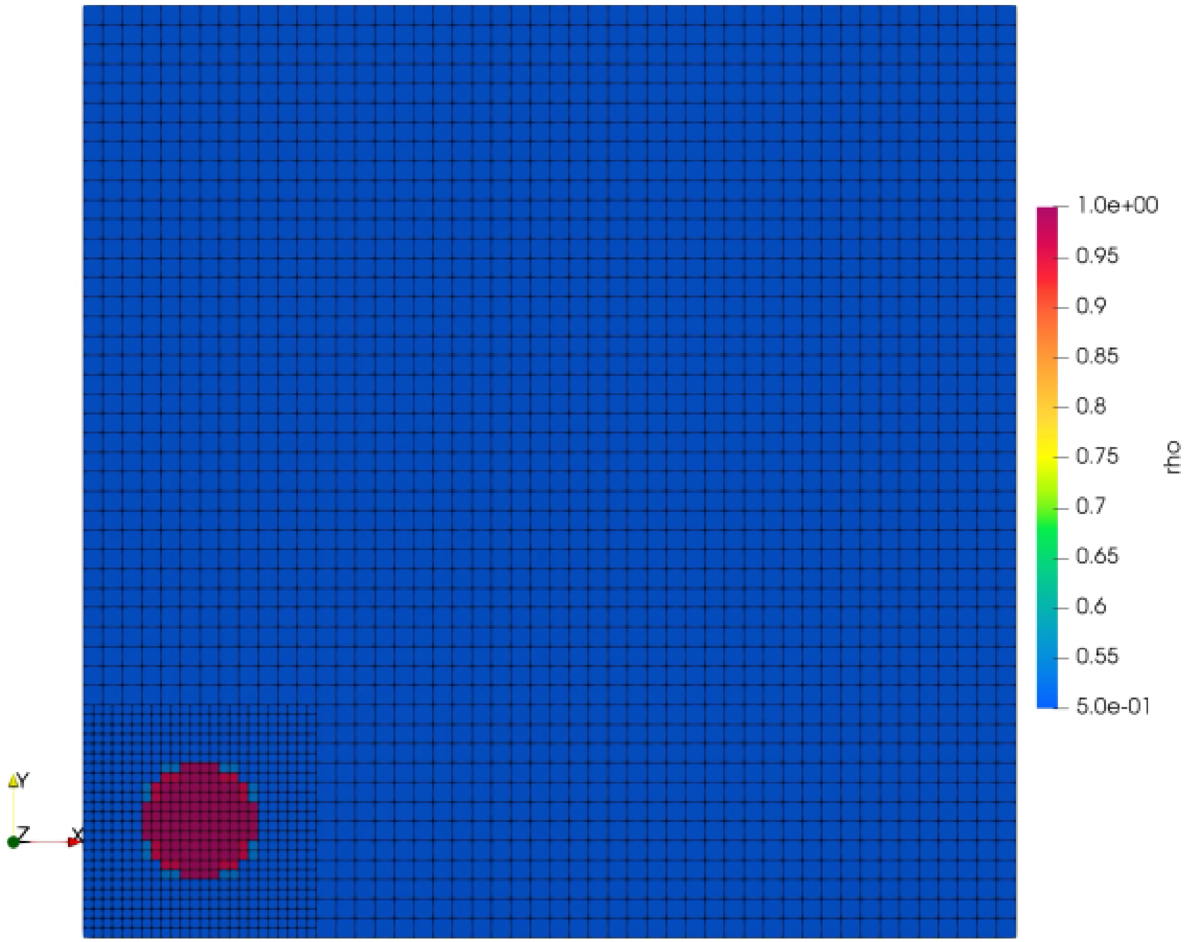

- Dynamic adaptivity
- Can capture fine-scale features of problems while remaining computationally feasible
- Refinement/coarsening criteria can be user-defined
  - Driven by error estimates
  - Driven by geometrical considerations
  - Driven by shock-capturing logic

https://github.com/sandialabs/DGTile

DGTile – Simple AMR Examples

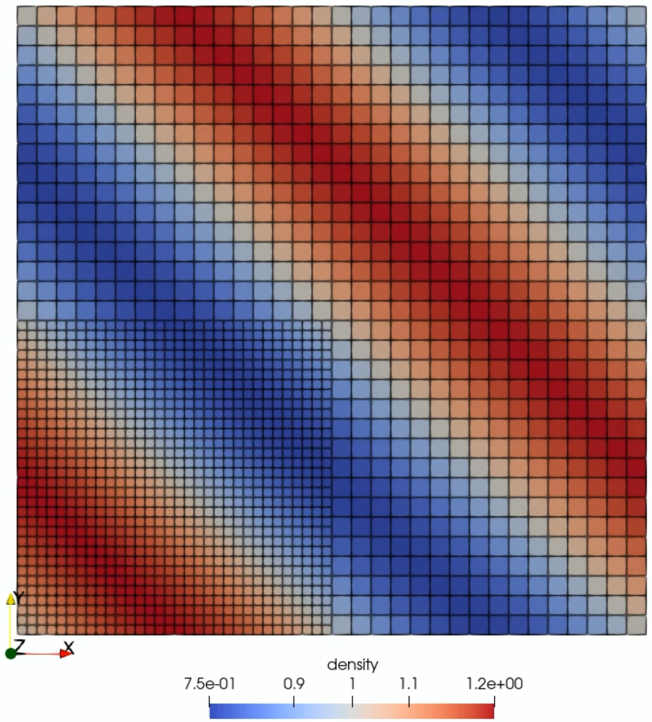

Advection through AMR mesh

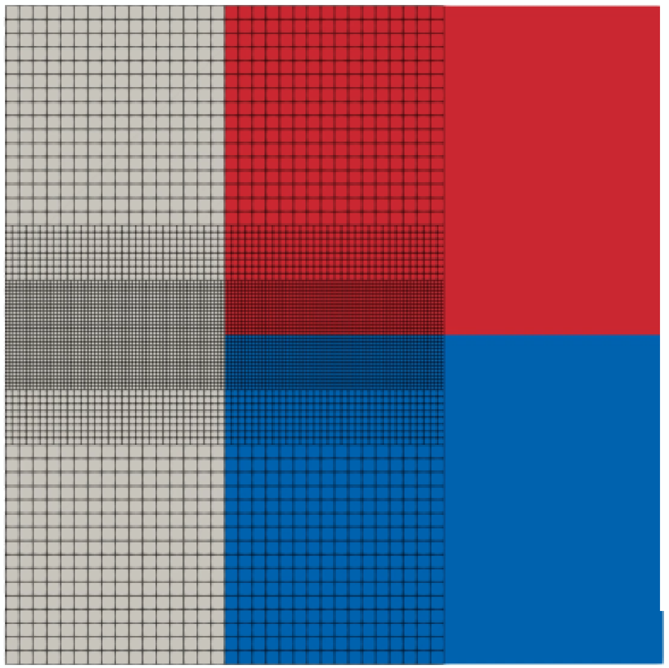

Adaptive Rayleigh-Taylor instability

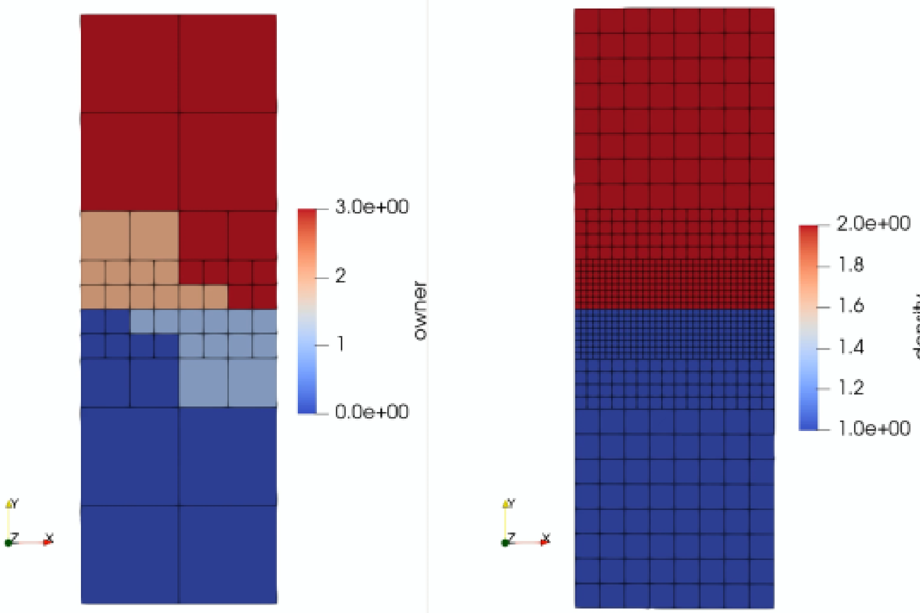

Load-balancing during Rayleigh-Taylor simulation

https://github.com/sandialabs/DGTile

Verification hierarchy includes standard multi-dimensional tests that are used to probe mesh refinement approaches

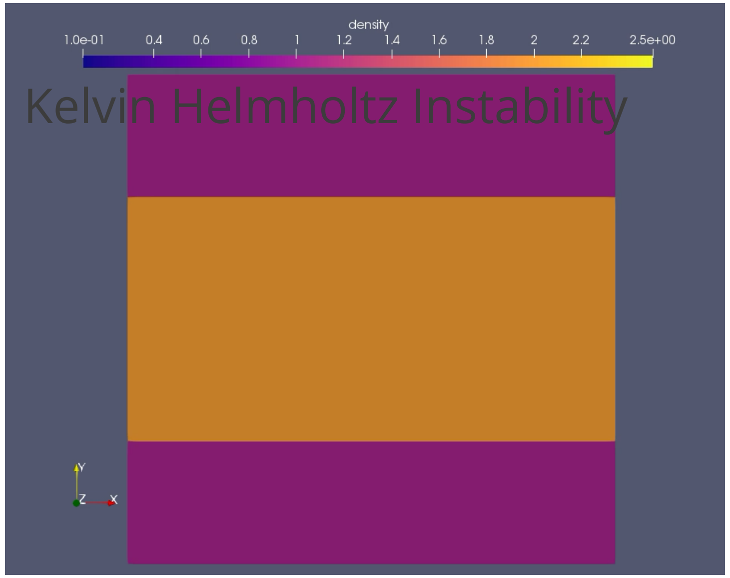

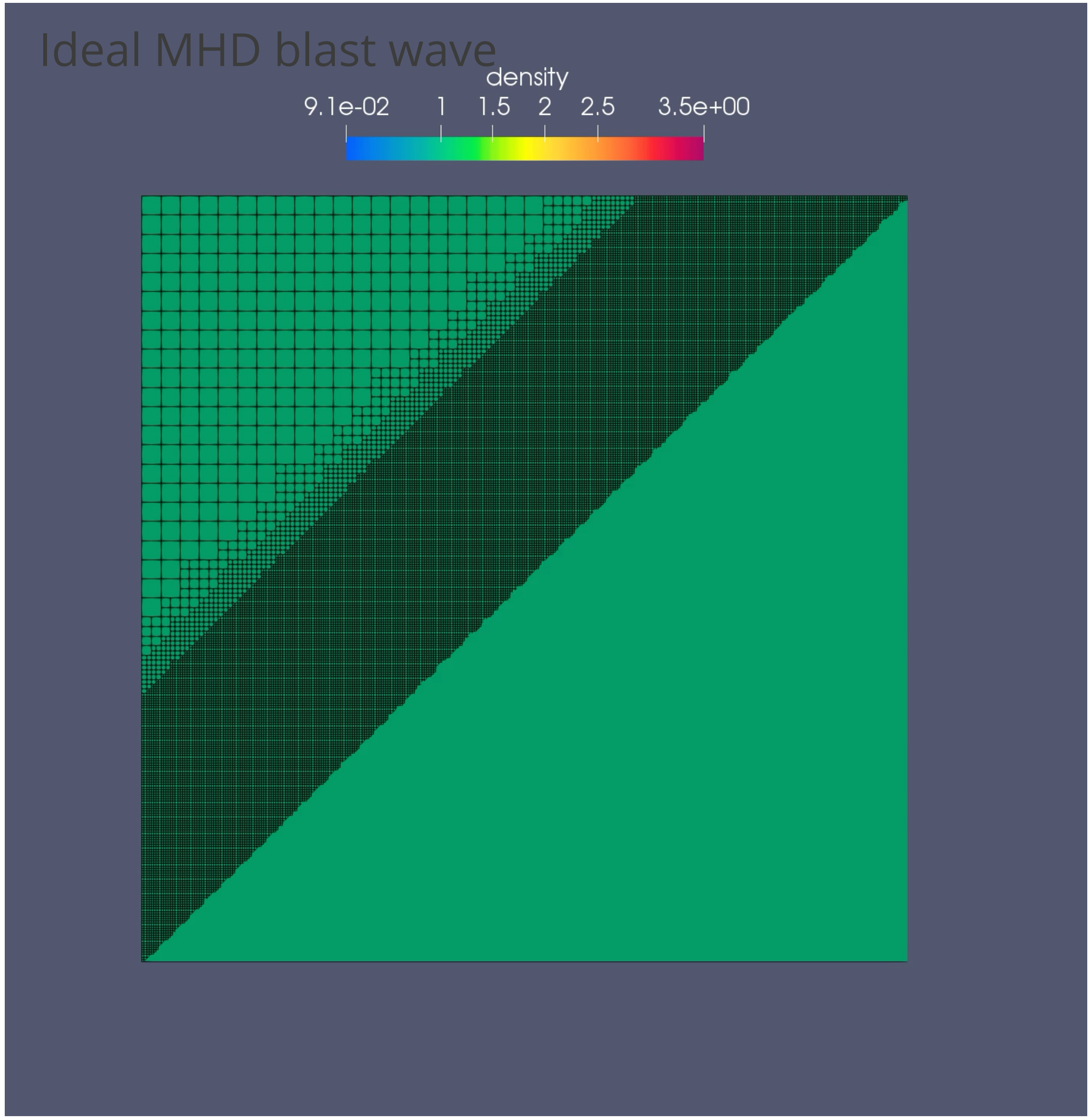

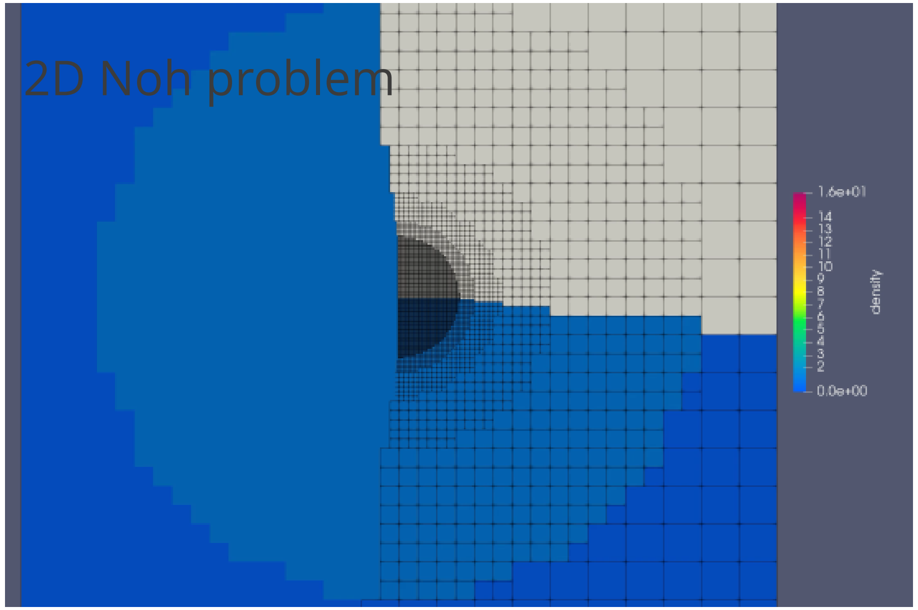

AMR + GPU allows us to dramatically improve time-to-solution to enable a design capability

- Magnetically driven implosion
  - 80x80x40 cells in uniform grid cases
  - Cylinder with sinusoidally perturbed surface
  - Poynting inflow, momentum outflow

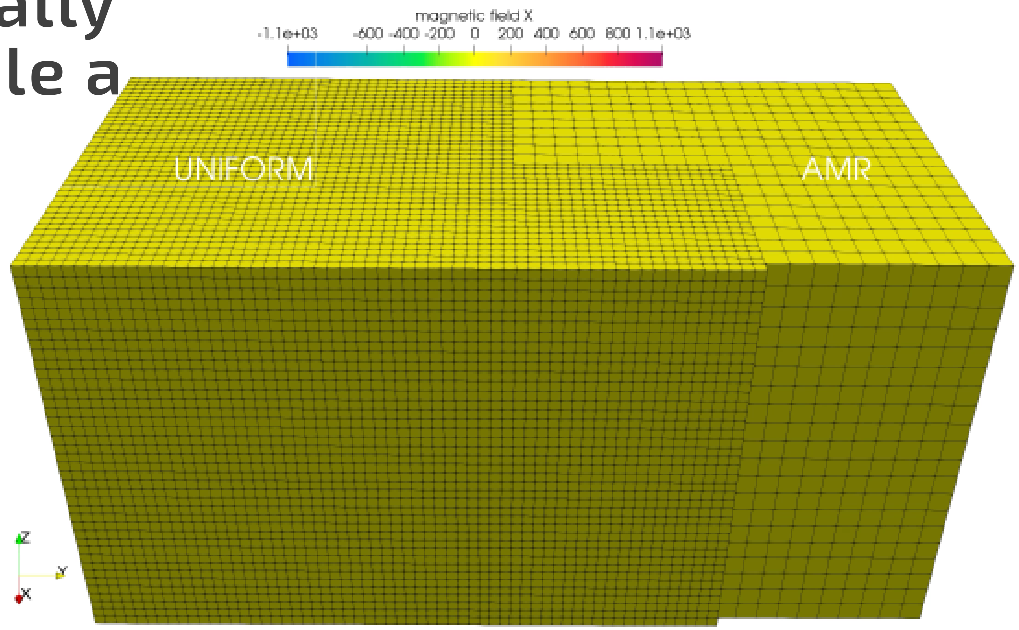

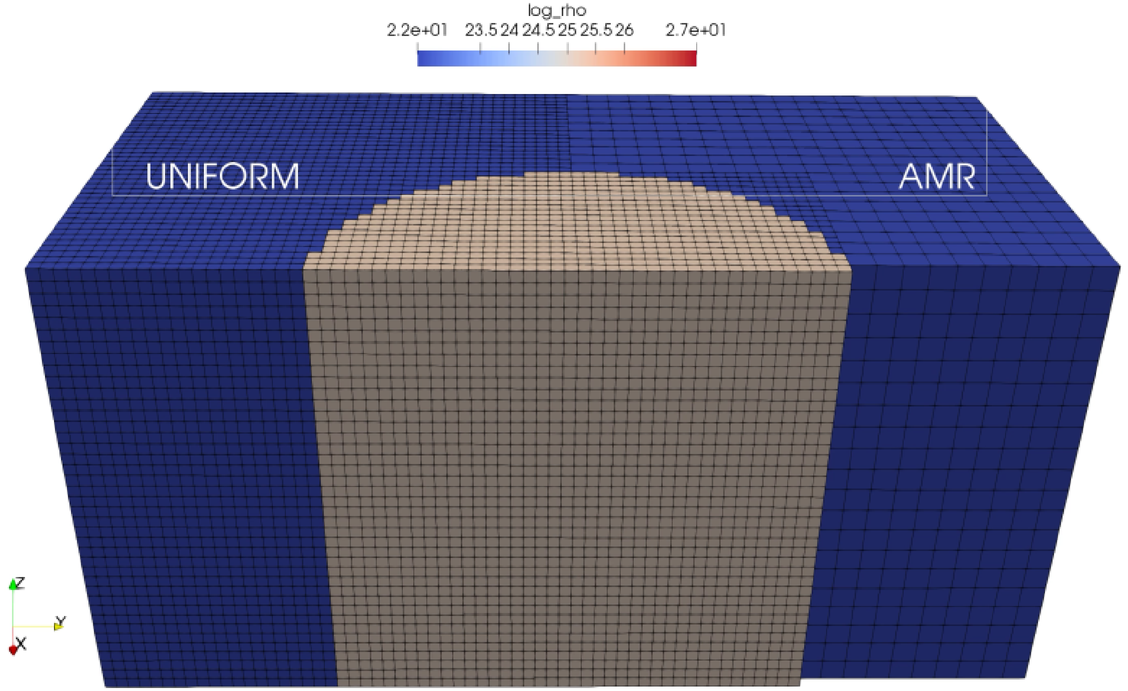

SMR (static mesh refinement) results agree nicely to uniform grid results

Table 1: Cylindrical Implosion Timings (80x80x80 cells, 10 steps)

PERSEUS	FLEXO
Intel(R) Xeon(R) CPU E7-4880	Tesla V100-SXM2-16GB
343.935s	2.177s

158 times faster!

DGTile enables mesh refinement to target geometries and rapidly decreases computational costs

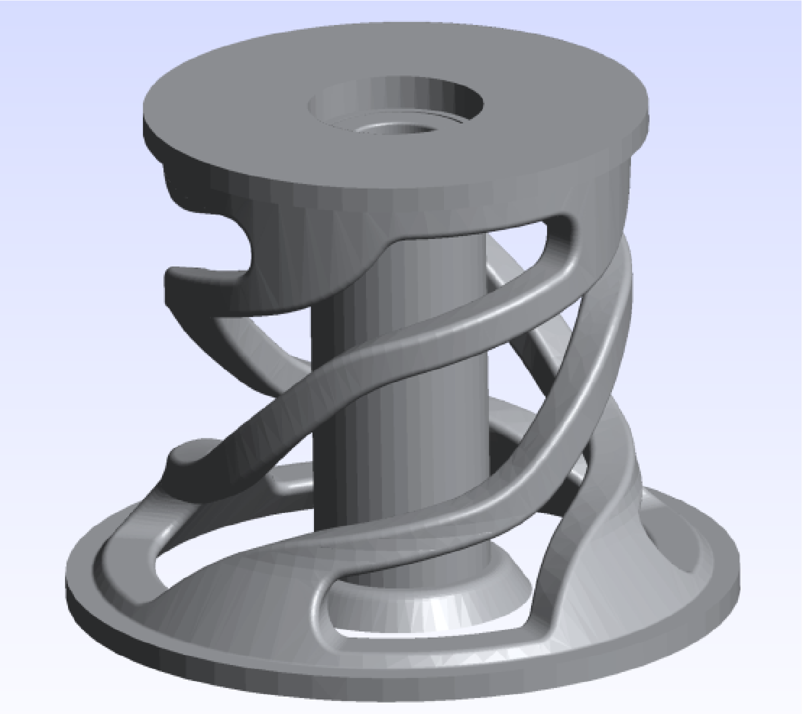

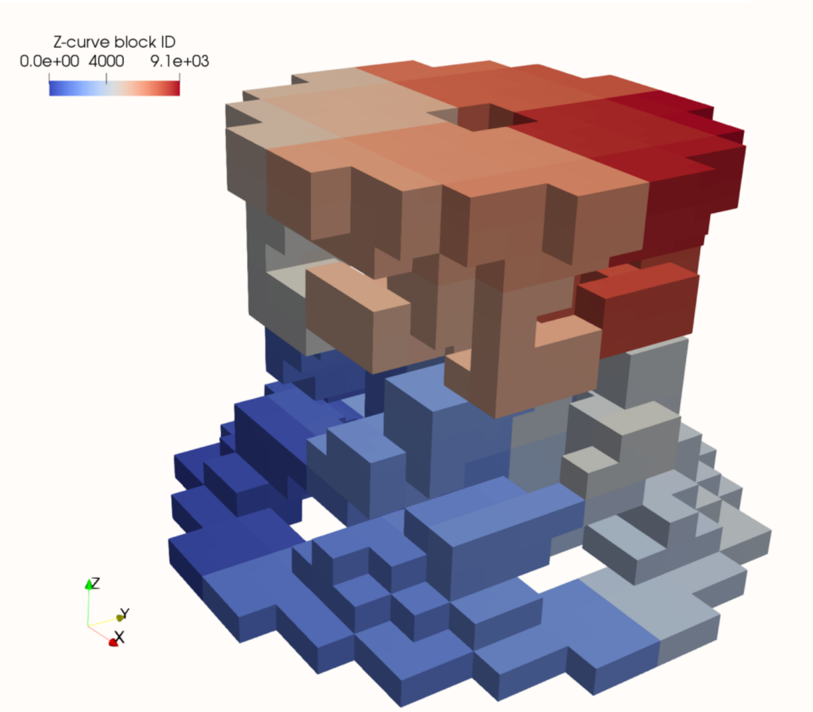

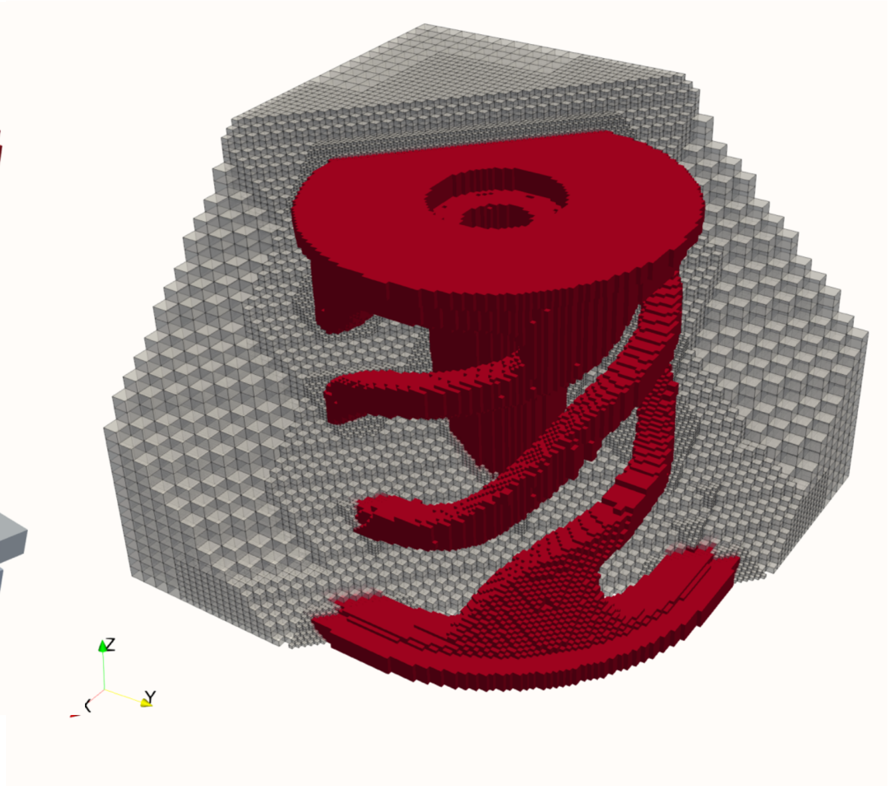

STL “CAD” geometry → Octree refined to STL geometry definition → Material initialization in refined octree mesh

- Target design problem with screw pinch geometry
  Desired resolution 1000x1000x1000 cells to resolve fine scales
  Current PERSEUS runs would require 20-30 THOUSAND cores
  Designers need to run AT LEAST 10 simulations!
  NOT computationally tractable

- With AMR shown above (just 6 levels of refinement)
  - Same resolution with 16x16x16 blocks
  - Leads to less than 4 million cells
  - Can be run on 80 cores

https://github.com/sandialabs/DGTile

FLEXO produces helical Magneto-Rayleigh-Taylor instability without the need for initial seeding

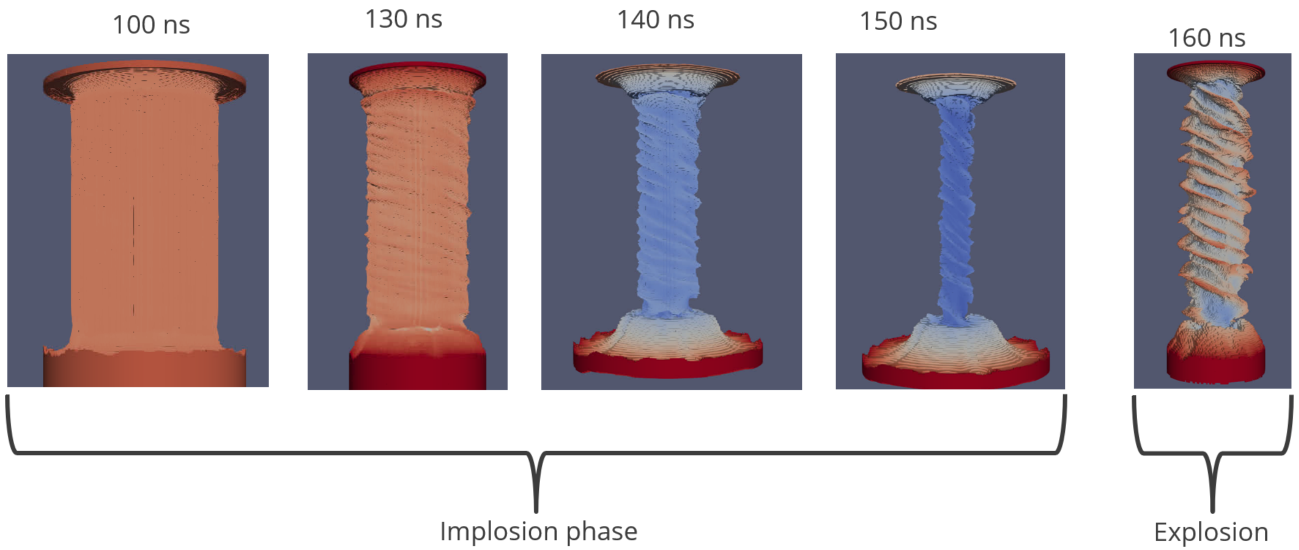

Azimuthal current density perturbation plotted at 140 ns

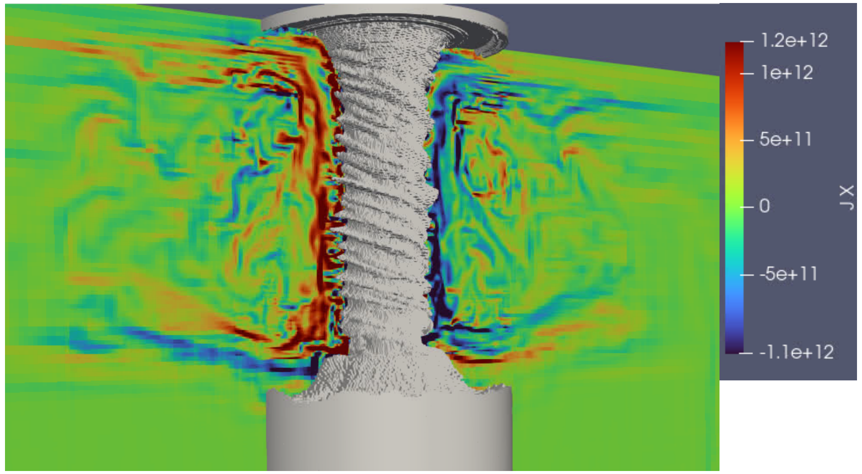

Helical magnetic fields at 140 ns due to flux compression

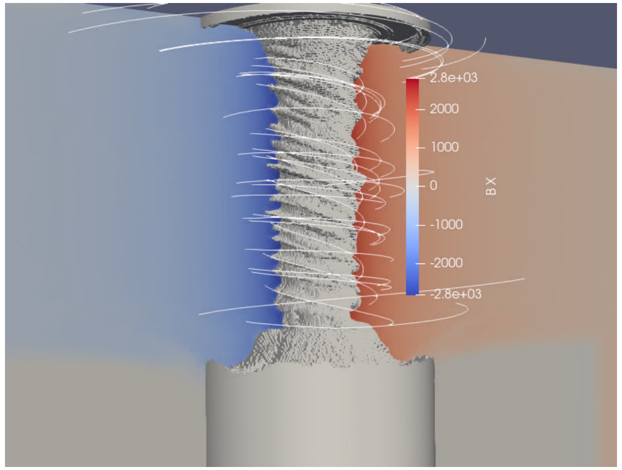

- Hall physics driven perturbations in the azimuthal current provide a seeding mechanism
- This has been observed in 1-Ma liner simulations (Woolstrum et al., 2022)
- Flux compression leading to late-time helical magnetic fields from low-density plasma also observed

Slide courtesy of Jeff Woolstrum

Exciting work is taking place at SNL in (X)MHD research with great opportunities for collaboration!

- We have unique validation data that can be used to understand algorithm fidelity
  - There are unanswered questions about the physics at work in our experiments
- We are developing new capabilities for XMHD to investigate these capabilities and developing rigorous verification hierarchies to demonstrate algorithm correctness
- We are creating production tools that are aimed at providing a fast, performance portable design tool:
  - "Productionizing" established XMHD algorithms
  - Developing and demonstrating a portably performant (MPI + X) AMR framework
  - Including tabular equations of state for material response
  - Extending single material XMHD formulation to a 6-equation multi-material model
  - Verification tests integrated with the development cycle using modern software tools and practices.
- Initial studies of 3D MagLIF implosions indicate that we are able to generate helical MRTI self-consistently using FLEXO